

6. A. V. Lykov, Heat and Mass Exchange [in Russian], Moscow (1972).
7. P. A. Novikov and V. A. Eremenko, Inzh.-Fiz. Zh., 23, No. 5 (1972).
8. P. Ya. Nedviga, G. Ya. Gridasov, and S. I. Kulikovskii, Priborostroenie, No. 15 (1973).
9. A. V. Lykov, Z. P. Shul'man, et al., Inzh.-Fiz. Zh., 22, No. 2 (1972).

## PERFORMANCE OF FILM COOLING BY INJECTION FROM A POROUS SECTION

V. M. Polyayev, E. E. Lyagushin, and Yu. M. Baskakov

UDC 536.244

Results are presented on film cooling by homogeneous injection into a turbulent boundary layer through porous inserts of various lengths along the main flow direction.

It is usual [1] to use the temperature of a thermally insulated wall in conjunction with the ordinary equation of heat transfer in calculating the parameters of elements working under conditions of severe heat loading and cooled by gas injection. The performance parameter for the film cooling may serve to characterize the adiabatic wall temperature, and this can be defined as

$$\eta = \frac{T_0 - T_{a.w}}{T_0 - T_1} \quad (1)$$

It is usual to apply correction factors to this performance parameter in order to incorporate the effects of factors such as the physicochemical characteristics of the two flows, the deviation from isothermal conditions, the compressibility, and so on, all of which substantially affect the heat transfer.

Results have been given [2-5] from measurements on the cooling performance behind porous elements used in such injection; however, the results correspond in the main to conditions under which there is very extensive injection through the porous surface, and hence the main flow is repelled from the surface.

On the other hand, considerable interest attaches to the use of such porous sections when the injection parameters are medium or small ( $m \leq 10^{-2}$ ).

Here we report measurements on the performance of gas injection through porous sections of various length along the flow direction for a wide range of injection parameters.

The system was built around a rectangular wind tunnel; Fig. 1 shows the working section. The working channel had a cross section of 90 × 90 mm and was made of lucite. The lower wall of the working part consisted of the model. The porous plate block 6 was of sealed construction, and one wall bore the porous plate with Chromel-Copel thermocouples emerging on the hot surface, which were made of wire of diameter 0.2 mm. The porous plates were made by rolling stainless steel wire mesh. The effective porosity of such plates was about 30%.

We used three such porous blocks, which were similar in design but differed in length along the flow direction: L = 380, 190, and 40 mm.

The porous section was preceded by a water-cooled part 5; this served to maintain a constant surface temperature on the impermeable part and also a largely constant temperature on the porous section.

The thermally insulated plastic plate 7 was 30 mm thick and of length 1 m; temperature transducers were set up on this surface with a pitch of 10 mm, and these consisted of small copper sections fitted with the Chromel-Copel thermocouples 8.

---

Bauman Higher Technical College, Moscow. Translated from Inzhenerno-Fizicheskii Zhurnal, Vol. 29, No. 5, pp. 793-798, November, 1975. Original article submitted December 20, 1974.

*This material is protected by copyright registered in the name of Plenum Publishing Corporation, 227 West 17th Street, New York, N.Y. 10011. No part of this publication may be reproduced, stored in a retrieval system, or transmitted, in any form or by any means, electronic, mechanical, photocopying, microfilming, recording or otherwise, without written permission of the publisher. A copy of this article is available from the publisher for \$7.50.*

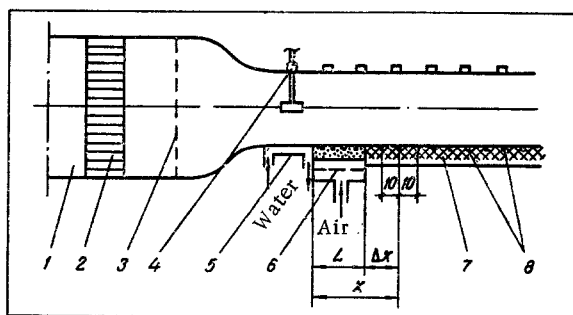


Fig. 1. Test section: 1) source; 2) equalizing grid; 3) grids; 4) probe tubes; 5) cooled plate; 6) porous plate; 7) insulated plate; 8) temperature sensors.

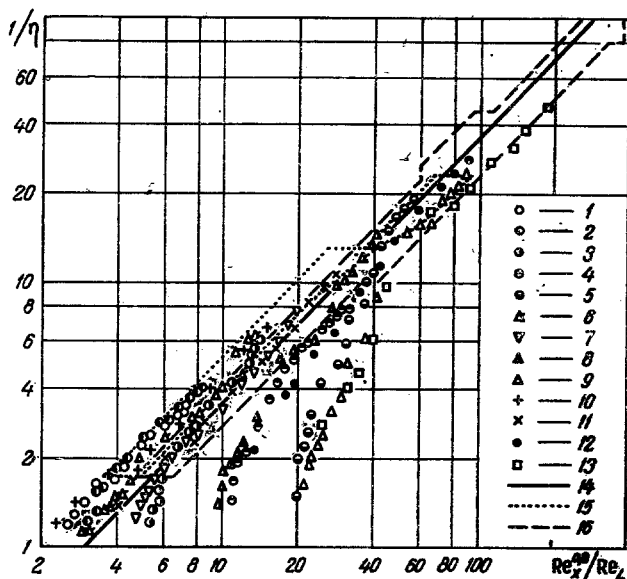


Fig. 2. Relation of  $1/\eta$  to  $Re_x^{0.8}/Re_L$ : 1-13) see Table 1; 14) from (2); 15) range of measurements in [2]; 16) the same for [4].

TABLE 1. Basic Working Characteristics

Working symbol No.	$m \cdot 10^3$	$U_0 \rho_0$ , kg /m <sup>2</sup> sec	$L \cdot 10^3$ , m	$\theta$
1	25,1	89,5	380	1,36
2	18,2	99,3	380	1,29
3	11,4	84,4	380	1,24
4	5,16	99,2	380	1,22
5	2,89	91	380	1,15
6	22,4	103,2	190	1,31
7	14,4	93,2	190	1,29
8	6,95	105,8	190	1,22
9	3,24	93,7	190	1,14
10	39	98,4	40	1,35
11	25,3	102,1	40	1,35
12	7,76	97,9	40	1,23
13	4,15	94,2	40	1,19

The air at the inlet to the working part had a temperature between 80 and 110°C; the injected air was supplied to the porous section from an independent cylinder, which also had means for adjusting the temperature and flow rate.

Measurements were made on the temperature and speed at the core of the main flow, as well as on the mass flow rate in the injected flow, the temperature distribution on the hot surface

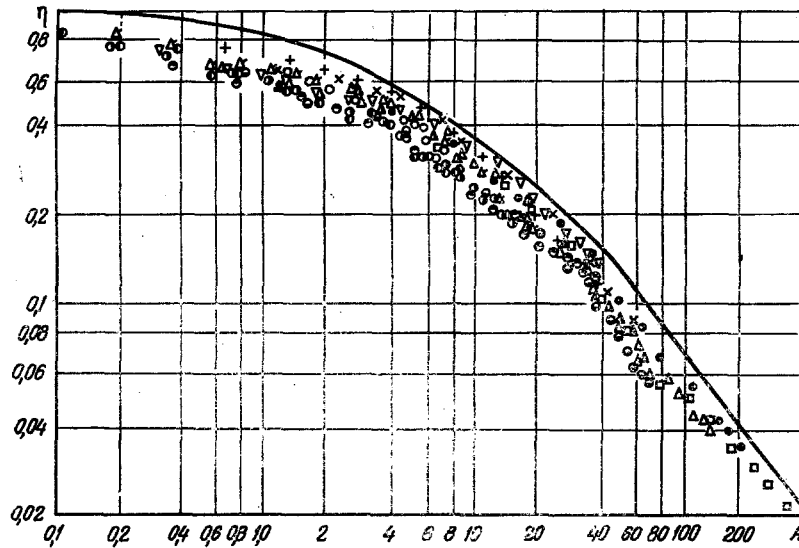


Fig. 3. Fit of results to (3):  $A = Re_{\Delta x} / Re_L^{1.25} [(T_0 - T_s) / (T_0 - T_1)]^{1.25}$ .

of the porous wall, and the same on the insulated wall. The emfs of the thermocouples were measured with a PP-63 potentiometer of accuracy class 0.05. All the measurements were made with the system in the steady state.

Preliminary measurements were made on the parameters of the boundary layer with Pitot tubes, which showed that a turbulent boundary layer was present whose effective start lay about 0.4 m from the leading edge of the porous plate.

The turbulence in the main flow was determined from the pulsation in the axial component of the velocity using an ETAM-ZA thermoanemometer in conjunction with the ESU amplifier from the ETAM-ZA, the result being about 0.025-0.030. Table 1 gives the basic parameters used in the tests.

Figure 2 shows the results in terms of  $Re_x^{0.8} / Re_L$  as parameter; this quantity has been used elsewhere [1, 2], and in the figure it is used in conjunction with the experimental data of [2, 4], which have been fitted to the limiting relationship

$$\frac{1}{\eta} = 0.33 \frac{Re_x^{0.8}}{Re_L}, \quad (2)$$

which was suggested in [1].

Figure 2 shows that our results agree satisfactorily with the published evidence at high rates of injection, and also with (2); however, at medium and low injection rates our values deviate from (2), and the deviation increases as the porous plate is approached.

Another expression has been suggested [1] for the performance of such a plate:

$$\eta = \left[ 1 + 0.25 \frac{Re_{\Delta x}}{Re_L^{1.25} \left( \frac{T_0 - T_s}{T_0 - T_1} \right)^{1.25}} \right]^{-0.8}. \quad (3)$$

Figure 3 compares our results with (3); it is clear that there is a tendency for the results to group not only in accordance with the injection parameter  $m$  but also with the length of the porous section. The results that fit best to (3) are those for the short porous section ( $L = 40$  mm), while those for the longest porous section show the largest deviation (about 30-50%), and this applies for the entire range of  $m$ , the values falling below the theoretical curve.

The results were further processed to show that a satisfactory unified relationship is

$$\eta = \frac{17.2m^{0.8}}{h^{0.8}} + \frac{1 - 17.2m^{0.8}}{h^5}. \quad (4)$$

Quantities such as the first term on the right in (4) have also been used in describing experimental results elsewhere [3, 5]; however, the performance figures obtained for  $m < 10^{-2}$  considerably exceed the values calculated in that way, particularly in the near region.

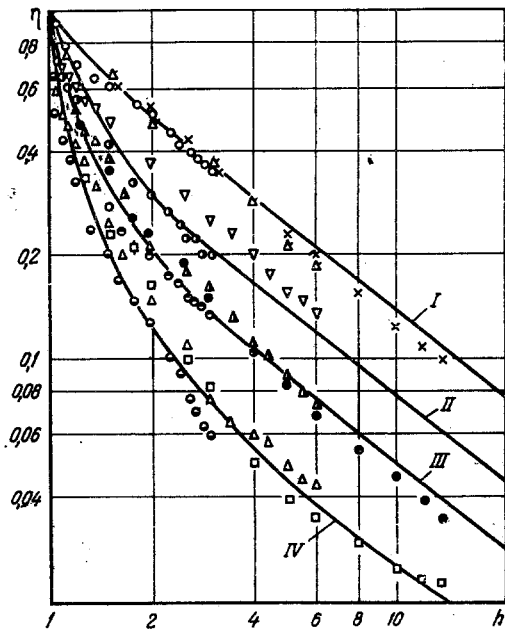


Fig. 4. Variation in performance factor along zone at various secondary injection rates: I-IV) calculated from (4): I)  $m = 25 \cdot 10^{-3}$ ; II)  $m = 12 \cdot 10^{-3}$ ; III)  $m = 7 \cdot 10^{-3}$ ; IV)  $m = 3 \cdot 10^{-3}$ . Symbols for measurements as in Fig. 2.

Figure 4 compares values calculated from (4) with experiment; the calculations were performed for four injection speeds. Correspondingly, the experimental data split up into four groups. It is clear that (4) describes the results satisfactorily for injection through porous sections of various lengths for a wide range in the injection parameters.

#### NOTATION

$T$ , temperature,  $^{\circ}\text{K}$ ;  $m$ , ratio of mass flow rates of injected and main flows through unit area;  $U$ , flow velocity,  $\text{m}/\text{sec}$ ;  $\rho$ , density,  $\text{kg}/\text{m}^3$ ;  $L$ , length of porous section,  $\text{m}$ ;  $\text{Re}_x$ , Reynolds number calculated from parameters of the main flow and current coordinate  $x$ ;  $\text{Re}_L$ , Reynolds number calculated by injection parameters;  $\mu$ , dynamic viscosity,  $\text{N}\cdot\text{sec}/\text{m}^2$ ;  $\theta$ , temperature parameter;  $h$ , length parameter. Indices: 0, main flow parameters; 1, parameters on porous surface; s, parameters of injected flow; aw, adiabatic wall parameters.

#### LITERATURE CITED

1. S. S. Kutateladze and A. I. Leont'ev, *Teplofiz. Vys. Temp.*, 1, No. 2 (1963).
2. N. Nishiwaki, M. Hirata, and A. Tsuchida, "International developments in heat transfer," *Amer. Soc. Mech. Eng.*, 4, 675 (1961).
3. R. Goldshein, H. Shewit, and T. S. Chen, *Teploperedacha*, 87, No. 3 (1965).
4. V. P. Komarov and A. I. Leont'ev, *Teplofiz. Vys. Temp.*, 8, No. 2 (1970).
5. P. N. Romanenko and A. Ya. Voloshchuk, *Teplofiz. Vys. Temp.*, 8, No. 5 (1970).